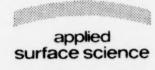


Applied Surface Science 231-232 (2004) ix-xviii



www.elsevier.com/locate/apsusc

Contents

Pretace	1
1. Plenary Session	
Challenges in localized high precision isotope analysis by SIMS G. Slodzian	3
Collisions of organic ions at surfaces R. Graham Cooks, SC. Jo and J. Green	13
2. Fundamentals	
Sputtering simulations of organic overlayers on metal substrates by monoatomic and clusters projectiles Z. Postawa	22
Molecular dynamics simulation of silicon sputtering: sensitivity to the choice of potential B.J. Thijsse, T.P.C. Klaver and E.F.C. Haddeman	29
A comparison of molecular dynamic simulations and experimental observations: the sputtering of gold {1 0 0} by 20 keV argon C.M. McQuaw, E.J. Smiley, B.J. Garrison and N. Winograd	39
Molecular dynamics simulations to explore the role of mass matching in the keV bombardment of organic films with polyatomic projectiles	
S. Harper and K.D. Krantzman Sputtering of a polycyclic hydrocarbon molecule: TOF-SIMS experiments and molecular dynamic simulations V. Solomko, A. Delcorte, B.J. Garrison and P. Bertrand	44
Cluster secondary ion mass spectrometry: an insight into "super-efficient" collision cascades R.D. Rickman, S.V. Verkhoturov and E.A. Schweikert	54
Energetic cluster induced desorption from a graphite surface R. Webb	59
Sputtering of Ag under C ₆₀ ⁺ and Ga ⁺ projectile bombardment S. Sun, C. Szakal, E.J. Smiley, Z. Postawa, A. Wucher, B.J. Garrison and N. Winograd	64
Molecular depth profiling in ice matrices using C ₆₀ projectiles A. Wucher, S. Sun, C. Szakal and N. Winograd	68
Emission of ionic water clusters from water ice films bombarded by energetic projectiles I.A. Wojciechowski, U. Kutliev, S. Sun, C. Szakal, N. Winograd and B.J. Garrison	72
Non-additive effects in secondary-ion emission from V, Nb and Ta under gold-cluster bombardment S.N. Morozov and U.Kh. Rasulev	78
Detection of the diatomic dications SiH ²⁺ and AlH ²⁺ K. Franzreb, R.C. Sobers Jr., J. Lörincík and P. Williams	82
Secondary ion emission from polycrystalline Al under Cs ⁺ irradiation P.A.W. van der Heide	86

P.A.W. van der Heide, C. Lupu, A. Kutana and J.W. Rabalais	90
Positive ionization probabilities of sputtered Ag and Ta clusters V. Kh. Ferleger	94
Secondary ion emission and work function measurements over the transient region from n and p type Si under Cs ⁺ irradiation	
P.A.W. van der Heide	97
On the trends in kinetic energies of secondary ions produced by polyatomic ion bombardment I.V. Veryovkin, S.F. Belykh, A. Adriaens, A.V. Zinovev and F. Adams	101
Characterization of surface structure by cluster coincidental ion mass spectrometry R.D. Rickman, S.V. Verkhoturov, S. Balderas, N. Bestaoui, A. Clearfield and E.A. Schweikert	106
Nanodomain analysis via coincidence ion mass spectrometry S.V. Verkhoturov, R.D. Rickman, S. Balderas and E.A. Schweikert	113
Detection of sputtered molecular doubly charged anions: a comparison of secondary-ion mass spectrometry (SIMS) and accelerator mass spectrometry (AMS) H. Gnaser, R. Golser, W. Kutschera, A. Priller, P. Steier and C. Vockenhuber	117
Emission processes of molecule-metal cluster ions from self-assembled monolayers of octanethiols on gold and silver B. Arezki, A. Delcorte and P. Bertrand	122
Positive secondary ion yield enhancement of metal elements using trichlorotrifluoroethane and tetrachloroethene backfilling	127
P.H. Chi and G. Gillen	127
Desorption/ionization of molecular nanoclusters: SIMS versus MALDI A. Delcorte, S. Hermans, M. Devillers, N. Lourette, F. Aubriet, JF. Muller and P. Bertrand	131
Imaging by atomic force microscopy of the electrical properties difference of the facets of oxygen-ion-induced ripple topography in silicon B. Gautier, B. Fares, G. Prudon and JC. Dupuy	136
Laboratory teaching of SIMS to university undergraduates R.J. Chater and D.S. McPhail	141
3. Cluster and Molecular Ion Beams	
C ₆₀ cluster ion bombardment of organic surfaces D.E. Weibel, N. Lockyer and J.C. Vickerman	146
Cluster primary ion bombardment of organic materials F. Kollmer	153
ToF-SIMS imaging with cluster ion beams J. Xu, S. Ostrowski, C. Szakal, A.G. Ewing and N. Winograd	159
Investigation of secondary cluster ion emission from self-assembled monolayers of alkanethiols on gold with ToF- SIMS	
M. Schröder, S. Sohn and H.F. Arlinghaus	164
Impact energy dependence of SF ₅ ⁺ ion beam damage of poly(methyl methacrylate) studied by time-of-flight secondary ion mass spectrometry M.S. Wagner and G. Gillen	169
Dynamic SIMS utilizing SF ₅ ⁺ polyatomic primary ion beams for drug delivery applications C.M. Mahoney, S. Roberson and G. Gillen	174
Depth profiling studies of multilayer films with a C ₆₀ ⁺ ion source A.G. Sostarecz, S. Sun, C. Szakal, A. Wucher and N. Winograd	179
C ₆₀ molecular depth profiling of a model polymer C. Szakal, S. Sun, A. Wucher and N. Winograd	183

Automated analysis of organic particles using cluster SIMS G. Gillen, C. Zeissler, C. Mahoney, A. Lindstrom, R. Fletcher, P. Chi, J. Verkouteren, D. Bright, R.T. Lareau and M. Boldman	186
Sputtering of indium using polyatomic projectiles A.V. Samartsev and A. Wucher	191
Polyatomic primary ion bombardment of organic materials: experiences in routine analysis B. Hagenhoff, K. Pfitzer, E. Tallarek, R. Kock and R. Kersting	196
Evaluation of a gold LMIG for detecting small molecules in a polymer matrix by ToF-SIMS S.R. Bryan, A.M. Belu, T. Hoshi and R. Oiwa	201
4. Organic Materials and Polymers	
Re-discovering surface mass spectrometry: chemical mapping from micro to macro K.G. Lloyd and D.P. O'Keefe	207
Enhancing and automating TOF-SIMS data interpretation using principal component analysis S.J. Pachuta	217
Organic molecule characterization—G-SIMS I.S. Gilmore and M.P. Seah	224
Multivariate statistical analysis of time-of-flight secondary ion mass spectrometry images using AXSIA J.A. Tony Ohlhausen, M.R. Keenan, P.G. Kotula and D.E. Peebles	230
Principal component analysis of TOF-SIMS spectra, images and depth profiles: an industrial perspective M.L. Pacholski	235
Optimal scaling of TOF-SIMS spectrum-images prior to multivariate statistical analysis M.R. Keenan and P.G. Kotula	240
Multivariate statistical analysis of time-of-flight secondary ion mass spectrometry images—looking beyond the obvious	
V.S. Smentkowski, J.A. (Tony) Ohlhausen, P.G. Kotula and M.R. Keenan	245
Interest of silver and gold metallization for molecular SIMS and SIMS imaging A. Delcorte and P. Bertrand	250
Organic SIMS: the influence of time on the ion yield enhancement by silver and gold deposition L. Adriaensen, F. Vangaever and R. Gijbels	256
Influence of primary ion bombardment conditions on the emission of molecular secondary ions R. Kersting, B. Hagenhoff, F. Kollmer, R. Möllers and E. Niehuis	261
Optimized conditions for selective gold flotation by ToF-SIMS and ToF-LIMS S.L. Chryssoulis and S.S. Dimov	265
Additive quantification on polymer thin films by ToF-SIMS: aging sample effects C. Poleunis, N. Médard and P. Bertrand	269
Characterization of poly(p-phenylene vinylene)/methanofullerene blends of polymer solar cells by time-of-flight secondary ion mass spectrometry C.W.T. Bulle-Lieuwma, J.K.J. van Duren, X. Yang, J. Loos, A.B. Sieval, J.C. Hummelen and R.A.J. Janssen	274
TOF-SIMS study of modified polymer surfaces Y. Lee, S. Han and MH. Kwon	274
Determination of oligomeric chain length distributions at surfaces using ToF-SIMS: segregation effects and polymer properties	
J.A. Gardella Jr. and C.M. Mahoney	283
ToF-SIMS molecular characterization and nano-SIMS imaging of submicron domain formation at the surface of PS/PMMA blend and copolymer thin films L. Kailas, JN. Audinot, HN. Migeon and P. Bertrand	289

Molecular weight evaluation of poly-dimethylsiloxane on solid surfaces using silver deposition/TOF-SIMS M. Inoue and A. Murase	296
Effect of deep UV (172 nm) irradiation on PET: ToF/SIMS analysis Z. Zhu and M.J. Kelley	302
Additive behavior in ultrathin polymer films investigated by ToF-SIMS N. Médard and P. Bertrand	309
ToF-SIMS investigation of functional mixed aromatic thiol monolayers on gold A. Auditore, N. Tuccitto, S. Quici, G. Marzanni, F. Puntoriero, S. Campagna and A. Licciardello	314
Static SIMS study of the behavior of K atoms on -CH ₃ , -CO ₂ H and -CO ₂ CH ₃ terminated self-assembled monolayers	210
Z. Zhu, B.C. Haynie and N. Winograd Aldehydes react with scribed silicon to form alkyl monolayers. Characterization by ToF-SIMS suggests an even-odd	318
effect YY. Lua, W.J.J. Fillmore and M.R. Linford	323
Layer-by-layer characterization of ultrathin films with secondary ion mass spectrometry Z. Li, R.D. Rickman, S.V. Verkhoturov and E.A. Schweikert	328
Investigation of fomblin Z-Dol end-groups on the magnetic recording disks by ToF-SIMS M. Ishikawa, Y. Osawa and O. Ishiwata	332
TOF-SIMS characterization of lubricants used in magnetic recording media B.C. Zhang, H.K. Liu and S. Chang	336
ToF-SIMS analysis of anti-fretting films generated on the surface of ball bearings containing dithiocarbamate and dithiophosphate grease additives	
R.G. Duque, Z. Wang, D. Duell and D.E. Fowler	342
A comparative study of carbocyanine dyes measured with TOF-SIMS and other mass spectrometric techniques L. Adriaensen, F. Vangaever and R. Gijbels	348
Depth profile analysis of chemically amplified resist by using TOF-SIMS with gradient shaving preparations N. Man, H. Okumura, H. Oizumi, N. Nagai, H. Seki and I. Nishiyama	353
Ga ⁺ TOF-SIMS lineshape analysis for resolution enhancement of MALDI MS spectra of a peptide mixture D.I. Malyarenko, H. Chen, A.L. Wilkerson, E.R. Tracy, W.E. Cooke, D.M. Manos, M. Sasinowski and O.J. Semmes	357
A ToF-SIMS study of linseed oil bonded to mercapto silane treated aluminium U. Bexell, M. Olsson, PE. Sundell, M. Johansson, P. Carlsson and M. Hellsing	362
5. Life Sciences	
Analysis of adsorbed proteins by static time-of-flight secondary ion mass spectrometry M.S. Wagner and D.G. Castner	366
Progress in cellular analysis using ToF-SIMS N.P. Lockyer and J.C. Vickerman	377
Quantitative TOF-SIMS imaging of DNA microarrays produced by bubble jet printing technique and the role of TOF-SIMS in life science industry	
H. Hashimoto, K. Nakamura, H. Takase, T. Okamoto and N. Yamamoto	385
Development of PNA microarrays for gene diagnostics with TOF-SIMS H.F. Arlinghaus, M. Schröder, J.C. Feldner, O. Brandt, J.D. Hoheisel and D. Lipinsky	392
ToF-SIMS characterization of hybridization onto self-assembled single-stranded DNA monolayers N.T. Samuel and D.G. Castner	397
ToF-SIMS surface and interface characterization of the immobilized camel antibody (cAb) onto SAMs-COOH/Au substrates	
A. Azioune, JJ. Pireaux and L. Houssiau	402

0	**
Contents	X11

Interpretation of static time-of-flight ion mass spectral images of adsorbed protein films on topographically complex surfaces S. Rangarajan and B.J. Tyler	400
TOF-SIMS imaging of protein adsorption on dialysis membrane S. Aoyagi, M. Hayama, U. Hasegawa, K. Sakai, T. Hoshi and M. Kudo	411
ToF-SIMS applied to probe bixin in <i>Bixa orellana</i> seeds L. Houssiau, M. Felicissimo, C. Bittencourt and J.J. Pireaux	416
ToF-SIMS studies as a tool to discriminate between spores and vegetative cells of bacteria C.E. Thompson, H. Jungnickel, N.P. Lockyer, G.M. Stephens and J.C. Vickerman	420
Molecule-specific imaging analysis of carcinogens in breast cancer cells using time-of-flight secondary ion mass spectrometry	
J.N. Quong, M.G. Knize, K.S. Kulp and K.J. Wu	424
Quantitative imaging of atomic and molecular species in cancer cell cultures with TOF-SIMS and Laser-SNMS M. Fartmann, C. Kriegeskotte, S. Dambach, A. Wittig, W. Sauerwein and H.F. Arlinghaus	428
Detection of protein immobilization on biosensor surfaces by TOF-SIMS S. Aoyagi, Y. Oiw and M. Kudo	432
Application of TOF-SIMS to monitor coating processes on biological and organic surfaces R. Chatterjee	437
Simultaneous determination of drug surface concentration and polymer degradation kinetics in biodegradable polymer/drug membranes: a model drug delivery system JW. Lee and J.A. Gardella Jr.	442
Rapid identification of phthalates in blood bags and food packaging using ToF-SIMS C.Y. Chen, A.V. Ghule, W.Y. Chen, C.C. Wang, Y.S. Chiang and Y.C. Ling	447
Imaging ToF-SIMS and synchrotron-based FT-IR microspectroscopic studies of prostate cancer cell lines E. Gazi, N.P. Lockyer, J.C. Vickerman, P. Gardner, J. Dwyer, C.A. Hart, M.D. Brown, N.W. Clarke and J. Miyan	452
Subcellular SIMS imaging of gadolinium isotopes in human glioblastoma cells treated with a gadolinium containing MRI agent	
D.R. Smith, D.R. Lorey II and S. Chandra	457
Subcellular SIMS imaging of isotopically labeled amino acids in cryogenically prepared cells S. Chandra	462
3D subcellular SIMS imaging in cryogenically prepared single cells S. Chandra	467
TOF-SIMS investigation of metallic material surface after culturing cells S. Aoyagi, S. Hiromoto, T. Hanawa and M. Kudo	470
Subcellular localization of aluminum and indium in the rat kidney P. Galle, R. Levi-Setti, A. Lamperti, K. Bourahla and F. Escaig	475
Ion microprobe imaging of ⁴⁴ Ca-labeled mammalian chromosomes R. Levi-Setti, K.L. Gavrilov, P.L. Strissel and R. Strick	479
Specific Mg ²⁺ binding at human and Indian muntjac chromosomal Giemsa bands P.L. Strissel, R. Strick, K.L. Gavrilov and R. Levi-Setti	485
Imaging of arsenic traces in human hair by nano-SIMS 50 JN. Audinot, S. Schneider, M. Yegles, P. Hallegot, R. Wennig and HN. Migeon	490
Accumulation of chromium in root tissues of <i>Eichhornia crassipes</i> (Mart.) Solms. in Cachoeira river—Brazil P.A.O. Mangabeira, L. Labejof, A. Lamperti, AA.F. de Almeida, A.H. Oliveira, F. Escaig, M.I.G. Severo, D. da C. Silva, M. Saloes, M.S. Mielke, E.R. Lucena, M.C. Martins, K.B. Santana, K.L. Gavrilov, P. Galle and	407
R. Levi-Setti	497
Influence of hydrocarbons on element detection in ion images by SIMS microscopy K. Takaya, M. Okabe, M. Sawataishi and T. Yoshida	502

Laser-SNMS analysis of apatite formation in vitro S. Dambach, M. Fartmann, C. Kriegeskotte, C. Brüning, H.P. Wiesmann, D. Lipinsky and H.F. Arlinghaus	506
6. Environmental Sciences	
Room temperature corrosion of museum glass: an investigation using low-energy SIMS S. Fearn, D.S. McPhail and V. Oakley	510
TOF-SIMS measurement for the complex particulate matter in urban air environment B. Tomiyasu, K. Suzuki, T. Gotoh, M. Owari and Y. Nihei	515
TOF-SIMS analysis of sea salt particles: imaging and depth profiling in the discovery of an unrecognized mechanism for pH buffering D.J. Gaspar, A. Laskin, W. Wang, S.W. Hunt and B.J. Finlayson-Pitts	520
ToF-SIMS analysis of atmospherically relevant sulphuric acid hydrate films and reactions thereof J.S. Fletcher and J.C. Vickerman	524
A comparative study on detection of organic surface modifiers on mineral grains by TOF-SIMS, VUV SALI TOF-SIMS and VUV SALI with laser desorption S.S. Dimov and S.L. Chryssoulis	528
ToF-SIMS as an alternative tool for the qualitative and quantitative analysis of polar herbicides M. Botreau, C. Guignard, L. Hoffmann and HN. Migeon	533
Application of a cryo-stage in the TOF-SIMS analysis of atmospheric aerosol surfaces A.P. Nair, B.J. Tyler and R.E. Peterson	538
7. Gate Dielectric Characterization	
Challenges for the characterization and integration of high-κ dielectrics R.M. Wallace	543
The influence of oxygen on the Hf signal intensity in the characterization of HfO ₂ /Si stacks C. Huyghebaert, T. Conard and W. Vandervorst	552
Analysis of high-k HfO ₂ and HfSiO ₄ dielectric films W. Nieveen, B.W. Schueler, G. Goodman, P. Schnabel, J. Moskito, I. Mowat and G. Chao	556
Quantification of nitrogen profiles in HfSiON films for gate dielectrics T. Yamamoto, T. Miyamoto and A. Karen	561
Sputter rate variations in silicon under high-k dielectric films J. Bennett, M. Beebe, C. Sparks, C. Gondran and W. Vandervorst	565
On the reliability of SIMS depth profiles through HfO ₂ -stacks W. Vandervorst, J. Bennett, C. Huyghebaert, T. Conard, C. Gondran and H. De Witte	569
ToF-SIMS profiling of HfO ₂ /Si stacks: influence of sputtering condition of profile shape T. Conard, C. Huyghebaert and W. Vandervorst	574
Nitrogen analysis in high-k stack layers: a challenge T. Conard, W. Vandervorst, H. De Witte and S. Van Elshocht	581
ToF-SIMS depth profiling of Hf and Al composition variations in ultrathin mixed HfO ₂ /Al ₂ O ₃ oxides L. Houssiau, R.G. Vitchev, T. Conard, W. Vandervorst and H. Bender	585
SIMS study on N diffusion in hafnium oxynitride D. Gui, J. Kang, H. Yu and H.F. Lim	590
Backside-SIMS profiling of dopants in thin Hf silicate film C. Hongo, M. Takenaka, Y. Kamimuta, M. Suzuki and M. Koyama	594
High resolution depth profiling of thin STO in high-k oxide material U. Ehrke, A. Sears, L. Alff and D. Reisinger	598

_	
Contents	XV

Depth profiling of ZrO ₂ /SiO ₂ /Si stacks—a TOF-SIMS and computer simulation study V.A. Ignatova, T. Conard, W. Möller, W. Vandervorst and R. Gijbels	603
Characterization of high-k dielectrics with ToF-SIMS S. Ferrari	609
Depth profiles of boron and nitrogen in SiON films by backside SIMS J. Sameshima, R. Maeda, K. Yamada, A. Karen and S. Yamada	614
8. Ultra Shallow Depth Profiling	
Errors in near-surface and interfacial profiling of boron and arsenic W. Vandervorst, T. Janssens, B. Brijs, T. Conard, C. Huyghebaert, J. Frühauf, A. Bergmaier, G. Dollinger, T. Buyuklimanli, J.A. VandenBerg and K. Kimura	618
Arsenic shallow depth profiling: accurate quantification in SiO ₂ /Si stack M. Barozzi, D. Giubertoni, M. Anderle and M. Bersani	632
Improved near surface characterization of shallow arsenic distribution by SIMS depth profiling T.H. Büyüklimanli, J.W. Marino and S.W. Novak	636
Toward accurate in-depth profiling of As and P ultra-shallow implants by SIMS A. Merkulov, E. de Chambost, M. Schuhmacher and P. Peres	640
Ultra-shallow arsenic implant depth profiling using low-energy nitrogen beams S. Fearn, R. Chater and D. McPhail	645
Evaluation of BN-delta-doped multilayer reference materials for shallow depth profiling in SIMS: round-robin test F. Toujou, S. Yoshikawa, Y. Homma, A. Takano, H. Takenaka, M. Tomita, Z. Li, T. Hasegawa, K. Sasakawa, M. Schuhmacher, A. Merkulov, H.K. Kim, D.W. Moon, T. Hong and JY. Won	649
Sub-keV secondary ion mass spectrometry depth profiling: comparison of sample rotation and oxygen flooding R. Liu and A.T.S. Wee	653
a-Si Capping SIMS for shallow dopant profiles S. Miwa	658
Site-specific SIMS backside analysis C. Gu, R. Garcia, A. Pivovarov, F. Stevie and D. Griffis	663
Backside and frontside depth profiling of B delta doping, at low energy, using new and previous magnetic SIMS instruments	
F. Laugier, J.M. Hartmann, H. Moriceau, P. Holliger, R. Truche and J.C. Dupuy	668
Accurate depth profiling for ultra-shallow implants using backside-SIMS C. Hongo, M. Tomita and M. Takenaka	673
Influence of surface orientation on the formation of sputtering-induced ripple topography in silicon B. Fares, B. Gautier, N. Baboux, G. Prudon, P. Holliger and J.C. Dupuy	678
O ₂ ⁺ versus Cs ⁺ for high depth resolution depth profiling of III–V nitride-based semiconductor devices M. Kachan, J. Hunter, D. Kouzminov, A. Pivovarov, J. Gu, F. Stevie and D. Griffis	684
Effects of crystalline regrowth on dopant profiles in preamorphized silicon M.J.P. Hopstaken, Y. Tamminga, M.A. Verheijen, R. Duffy, V.C. Venezia and A. Heringa	688
9. Silicon Germanium Characterization	
Energy and angular dependence of the sputter yield and ionization yield of Ge bombarded by ${\rm O_2}^+$ C. Huyghebaert, T. Conard and W. Vandervorst	693
SIMS depth profiling of SiGe:C structures in test pattern areas using low energy cesium with a Cameca IMS Wf M. Juhel and F. Laugier	698
Matrix effects in SIMS depth profiles of SiGe relaxed buffer layers F. Sánchez-Almazán, E. Napolitani, A. Carnera, A.V. Drigo, G. Isella, H. von Känel and M. Berti	704

Impact of the Ge concentration on the Ge-ionisation probability and the matrix sputter yield for a SiGe matrix under oxygen irradiation	
C. Huyghebaert, T. Conard, B. Brijs and W. Vandervorst	70
Use of SIMS in SiGe process control J.L. Maul, PF. Chou and Y.H. Lu	71
10. Semiconductors/Microelectronics	
Quantifying residual and surface carbon using polyencapsulation SIMS M. Beebe, J. Bennett, J. Barnett, A. Berlin and T. Yoshinaka	71
Quantification issues of trace metal contaminants on silicon wafers by means of TOF-SIMS, ICP-MS, and TXRF P. Rostam-Khani, M.J.P. Hopstaken, P. Vullings, G. Noij, O. O'Halloran and W. Claassen	720
Study on change in SIMS intensities near the interface between silicon-nitride film and silicon substrate T. Hasegawa, T. Date, A. Karen and A. Masuda	72:
Quantitative measurement of O/Si ratios in oxygen-sputtered silicon using ¹⁸ O implant standards R.C. Sobers Jr., K. Franzreb and P. Williams	729
Application of TXRF for ion implanter dose matching experiments M.R. Frost, M. French and W. Harris	734
Secondary ion mass spectrometry characterization of indium-implanted silicon wafers C. Blackmer-Krasinski and W.R. Morinville	738
Optimization of SIMS analyses performed in the MCs _x ⁺ mode by using an in situ deposition of Cs T. Wirtz and HN. Migeon	743
Cesium/xenon dual beam depth profiling with TOF-SIMS: measurement and modeling of M ⁺ , MCs ⁺ , and M ₂ Cs ₂ ⁺ yields	
J. Brison, T. Conard, W. Vandervorst and L. Houssiau	749
Cation Mass Spectrometer (CMS): recent developments for quantitative analyses of positive and negative secondary ions	
P. Philipp, T. Wirtz, HN. Migeon and H. Scherrer	754
Hydrogen redistribution in CVD SiO ₂ during post-oxidation annealing investigated by SIMS Y. Kawashima, H. Kawano, K. Terashima, K. Hamada, S. Aoyagi and M. Kudo	758
Sputtered depth scales of multi-layered samples with in situ laser interferometry: arsenic diffusion in Si/SiGe layers P.A. Ronsheim, R. Loesing and A. Madan	762
Short-term and long-term RSF repeatability for CAMECA SC-Ultra SIMS measurements M. Barozzi, D. Giubertoni, M. Anderle and M. Bersani	768
Front- and back-end process characterization by SIMS to achieve electrically matched devices T. Budri and D. Kouzminov	772
Effects of contamination on selective epitaxial growth B.J. MacDonald, E. Paton, E. Adem and B. En	776
Utilization of electron impact ionization of gaseous and sputtered species in the secondary ion acceleration region of a magnetic sector SIMS instrument A. Pivovarov, C. Gu, F. Stevie and D. Griffis	781
Improved charge neutralization method for depth profiling of bulk insulators using O_2^+ primary beam on a magnetic	701
sector SIMS instrument A.L. Pivovarov, F.A. Stevie and D.P. Griffis	786
SIMS study of Cu trapping and migration in low-k dielectric films Y. Li, J. Hunter and T.J. Tate	791
Optimization of SIMS analysis conditions for Na, S, P and N in Cu films Y. Li	796
1. 14	170

Contonts	979.74
Contents	XVI

Deconvolution analysis of dopant depth profile of Si at AlGaAs/GaAs interface using Al composition profile as reference	
Y. Kawashima, T. Ide, S. Aoyagi and M. Kudo	800
Copper-indium-gallium-diselenide/molybdenum layers analyzed by corrected SIMS depth profiles G. Bilger, P.O. Grabitz and A. Strohm	804
Characterization of light element impurities in gallium-nitride-phosphide by SIMS analysis R.C. Reedy, J.F. Geisz, A.J. Ptak, B.M. Keyes and W.K. Metzger	808
Characterization of silicon nanocrystals embedded in thin oxide layers by TOF-SIMS M. Perego, S. Ferrari, M. Fanciulli, G. Ben Assayag, C. Bonafos, M. Carrada and A. Claverie	813
Cluster ion emission from nitrogen-doped GaAs and optimization of SIMS conditions for nitrogen analysis G.M. Guryanov	817
Ti diffusion in chalcogenides: a ToF-SIMS depth profile characterization approach S.G. Alberici, R. Zonca and B. Pashmakov	821
Zinc determination in A ³ B ⁵ semiconductors K.D. Yu and A.P. Kovarsky	826
11. Materials Science	
The role of dynamic SIMS in process development for high-temperature superconducting wire R.E. Ericson	829
Oxygen isotopic tracer measurements in ceramics and ceramic composites with a fine focus gallium primary ion gun R.J. Chater and D.S. McPhail	834
TOF-SIMS study of pyridine intercalated nanorods of bismuth molybdate A.V. Ghule, CY. Chen, FD. Mei and YC. Ling	840
Reaction monitoring of polyaniline film formation on carbon nanotubes with TOF-SIMS WY. Chen, CY. Chen, KY. Hsu, CC. Wang and YC. Ling	845
ToF-SIMS depth profiling of alumina scales formed on a FeCrAl high-temperature alloy J. Engkvist, U. Bexell, T.M. Grehk and M. Olsson	850
Effect of low level contamination on TiAl alloys studied by SIMS O.M.N.D. Teodoro, J. Barbosa, M. Duarte Naia and A.M.C. Moutinho	854
SIMS analyses on Co:ns-C thin films A. Lamperti, K.L. Garvilov, R. Levi-Setti, G. Bongiorno, M. Blomqvist, P.M. Ossi and C.E. Bottani	859
Evaluation of oxygen in oxide materials by SIMS using ¹⁸ O ₂ gas S. Takeda	864
Characterization of nickel phosphorus surface by ToF-SIMS B.C. Zhang, G. Barth, H.K. Liu and S. Chang	868
12. Isotopic Ratio and Earth Sciences	
QSA influences on isotopic ratio measurements G. Slodzian, F. Hillion, F.J. Stadermann and E. Zinner	874
Achieving high reproducibility isotope ratios with the Cameca IMS 1270 in the multicollection mode M. Schuhmacher, F. Fernandes and E. de Chambost	878
Multi-correlation analyses of TOF-SIMS spectra for mineralogical studies C. Engrand, J. Lespagnol, P. Martin, L. Thirkell and R. Thomas	883
Cryogenic SIMS and its applications in the earth sciences M. Wiedenbeck, D. Rhede, R. Lieckefett and H. Witzki	888
FIB-SIMS analysis of micro-particle impacts on spacecraft materials returned from low-earth orbit S. Kettle, R.J. Chater, G.A. Graham, D.S. McPhail and A.T. Kearsley	893

SIMS analyses of Mg, Cr, and Ni isotopes in primitive meteorites and short-lived radionuclides in the early solar	
Y. Guan, G.R. Huss and L.A. Leshin	899
SIMS study of self-consisted fractionation of iron and titanium isotopes in ilmenites P.I. Didenko and A.A. Efremov	903
Silicon isotopic zoning in silicon crystals caused by the isotopic fractionation at the crystal-melt interface Y. Morishita and H. Satoh	907
Peak fitting to resolve CN ⁻ isotope ratios in biological and environmental samples using TOF-SIMS J.B. Cliff, D.J. Gaspar, P.J. Bottomley and D.D. Myrold	912
Using SIMS to diagnose color changes in heat treated gem sapphires S.W. Novak, C.W. Magee, T. Moses and W. Wang	917
13. Instrumentation	
SIMION modeling of ion optical effects in Cameca ion microanalyzers: simulation of ion transmission losses J. Lorincik, K. Franzreb and P. Williams	921
High-resolution primary ion beam probe for SIMS S.K. Guharay, S. Douglass and J. Orloff	926
Evaluation of the nano-beam SIMS apparatus M. Nojima, M. Toi, A. Maekawa, B. Tomiyasu, T. Sakamoto, M. Owari and Y. Nihei	930
The development of C_{60} and gold cluster ion guns for static SIMS analysis R. Hill and P.W.M. Blenkinsopp	936
Development of a column delivering a collimated stream of Cs ⁰ for SIMS purposes T. Wirtz and HN. Migeon	940
Development of compact cluster ion sources using metal cluster complexes. Ionization properties of metal cluster complexes	
T. Mizota, H. Nonaka, T. Fujimoto, A. Kurokawa and S. Ichimura	945
Latest developments for the CAMECA ULE-SIMS instruments: IMS Wf and SC-Ultra E. de Chambost, A. Merkulov, P. Peres, B. Rasser and M. Schuhmacher	949
Accurate on-line depth calibration with a laser interferometer during SIMS profiling on the Cameca IMS WF instrument	
A. Merkulov, O. Merkulova, E. de Chambost and M. Schuhmacher	954
Sample holder implement for very small samples on SC-ultra SIMS instrument M. Barozzi, D. Giubertoni, M. Sbetti, M. Anderle and M. Bersani	959
A new horizon in secondary neutral mass spectrometry: post-ionization using a VUV free electron laser I.V. Veryovkin, W.F. Calaway, J.F. Moore, M.J. Pellin, J.W. Lewellen, Y. Li, S.V. Milton, B.V. King and M. Petravić	962
Rapid characterisation of surface modifications and treatments using a benchtop SIMS instrument D.S. McPhail, M. Sokhan, E.E. Rees, B. Cliff, A.J. Eccles and R.J. Chater	967
High mass resolution SIMS S. Maharrey, R. Bastasz, R. Behrens, A. Highley, S. Hoffer, G. Kruppa and J. Whaley	972
Development of an instrument for simultaneous detection of positive and negative scanning ion images S. Seki, H. Tamura, T. Kanoh and T. Satoh	976
Author Index	III
Subject Index	XV